Y. Ras Mathew
B. Ganesh Babu

ISSN 1333-1124
ISSN 1849-1391

A REAL TIME EXPERIMENTAL SET UP TO ANALYSE AUTOMATIC ACTUATION OF A FIRE SPRINKLER USING A SHAPE MEMORY ALLOY (NITINOL)

Summary

A fire sprinkler system has to detect fire and actuate the sprinklers to discharge water automatically to put out the fire as soon as possible. Currently, when a fusible bulb fire sprinkler is exposed to fire, it opens and discharges water automatically but it is not able to stop the discharge of water when the fire is putout. This paper describes a newly designed Automatically Actuated Fire Sprinkler (AAFS) integrated with a NiTinol spring in which the Shape Memory Effect (SME) is utilized to actuate and de-actuate the fire sprinkler automatically. At ambient temperature, a small spring maintains the closed position of the AAFS. When the temperature rises above 88°C, the NiTinol spring actuates the AAFS to discharge water. When the fire is extinguished, the austenite phase of the NiTinol spring changes to the martensite phase and the spring returns back to its initial position. Thus, it automatically stops the water discharge and minimizes the water consumption without any control systems.

Key words: *NiTinol spring, Phase transformation, Shape memory effect*

1. Introduction

Major fire accidents take place due to carelessness, gas leakages, short circuits, overheating of electrical appliances, etc. During a fire accident, the fire should be put outas soon as possible to avoid losses of lives and properties. Nowadays, Halon fire extinguishing systems are replaced by fine water-spray systems to suppress fire even in areas involving electrical appliances [1]. Jinsong et al. investigated the effects of several important factors, such as water spray pattern, water droplet size, and water spray flow rate on the fire suppression mechanism and proved that the water spray with a solid cone pattern and a finer water droplet size is very effective in extinguishing fires [2]. Xiangyang et al. investigated experimentally the spatial distribution of water volume, flux, droplet size, and the velocity of a sprinkler spray, and proved that the spray is strongly influenced by the configuration of the sprinkler frame arms and the sprinkler deflector tines and slots [3]. Buddy Clayton Shipman introduced an X bracket valve design to automatically actuate the sprinkler at higher temperatures [4]. James R. Anderson designed a fusible eutectic alloy to actuate the sprinkler automatically [5]. Heinz S. Wolff introduced a disc made of a shape memory alloy to break the shutter glass of a fire sprinkler automatically [6]. George S. Polan provided a C shape band made of a shape memory alloy to release the control lever of a sprinkler at high temperatures [7]. Marthinus Cornelius uses a shape memory alloy element to break an associated frangible bulb automatically at high

temperatures to discharge water [8]. Alfred Johnson patented a temperature-activated valve for a conventional fire sprinkler utilizing a hyperelastic single-crystal shape memory alloy [9]. In the examples listed above, all fire sprinklers are actuated automatically at high temperatures to discharge water, but when the temperature decreases (the fire is put out) the discharge of water is not stopped automatically. To stop the discharge of unwanted water, Tom Goss introduced a removable casing for fire sprinklers [10]. Hochiki Kabushiki introduced a fusible alloy within a shape memory alloy. The fusible alloy helps to actuate the sprinkle and the shape memory alloy to deactivate the sprinkle automatically [11].

2. Shape memory alloys

Smart materials can sense any environmental change and respond to it in various dimensions [12]. Shape Memory Alloys (SMAs) have the ability to change their stiffness, natural frequency, damping, shape, and other mechanical characteristics in response to changes in temperature, magnetic field or electric field [13]. Among the SMAs, NiTinol (Nickel Titanium Naval Ordnance Laboratory) has the ability to recover its large deformation and high ultimate tensile strength by 2% strain (17 Kg/mm^2) [12]. In SMAs, the modulus of elasticity changes with respect to temperature, i.e. the elasticity of a SMA in the high temperature phase is up to four times larger than that of the low temperature phase. Therefore, the stiffness of the structure can vary by a factor of three to four times. Hence, an antagonistic force (pre-stress) will be created in the SMA structure [14]. SMAs possess a two way Shape Memory Effect (SME): it can remember one geometric shape at high temperatures and the other at low temperatures. During repeated heating and cooling, the SMA changes its shape between its corresponding high and low temperature shapes without the help of an external force [15]. The SME occurs due to a reversible thermo-elastic phase transformation between the parent phase (austenite) and the product phase (martensite) and the phase transformation occurs as a function of both stress and temperature. The strain rate has a stronger effect on the load-displacement response. The mechanical behaviour of NiTinol with various strain rates is experimentally tested using Tanak's model. Thermal effects due to the hysteresis loop and the transformation of latent heat greatly influence the mechanical behaviour [16]. G.Song, explained various methods of implementation of SMA actuators in the applications of the passive, active, and semi-active vibration control of civil structures [17]. S.M.T. Hashemi utilized the SME of SMAs to control the vibration of a simply supported beam [18]. S.John and M.Hariri did an experimental study on changing the natural frequency of a structure by NiTinol-based memory alloy wire on a plate [19]. It is critical to understand the heat transfer of SMAs due to thin wires, large strain heat activation, ambient environment, etc. Anupam Pathak introduced a non–invasive technique for calculating the convective coefficient of SMAs by employing the temperature induced transformation strain of SMAs to estimate the surface temperature [20].

2.1 Mechanical behaviour of NiTinol

Shape memory effect exhibits a large residual strain after loading and unloading, which can be fully recovered by raising the temperature of the material [21]. In shape memory alloys, the austenite-to-martensite transformation depicts the accommodation process called lattice invariant shear. It can be accomplished in two ways: slip and twinning. A shape memory element has four relevant temperatures. In the ascending order, these temperatures are as follows: martensite finish, martensite start, austenite start, austenite finish. A shape memory alloy exhibits a temperature hysteresis between its martensite and austenite phase transformation. Properties of shape memory alloys can be used to generate large stresses and strains but their rates are generally limited due to the time required for heating the material to attain the strain recovery. A rise in the ambient temperature subsequently induces actuation due to the phase transformation between martensite and austenite [22]. NiTinol possesses

high electrical resistivity; therefore, the material can be heated and subsequently activated by passing a direct current through it [23]. By reviewing different studies, one can conclude that the fire sprinkler system is able to sense the fire and actuate automatically. However, it may not deactivate to stop the discharge of water and it requires maintenance and a separate control system to control the flow of water when the fire is put out. In these studies, the shape memory effect of NiTinol is used to sense the temperature changes and also as an actuator for activating and deactivating the fire sprinkler automatically. Hence the name – automatically actuated fire sprinkler (AAFS).

3. Conceptual design of an AAFS

An automatic fire sprinkler consists of the main piston, small piston, main spring, small spring, NiTinol spring, 'O' rings, and deflector. The main piston controls the flow of water from the inlet to the deflector and the main spring helps to retain the initial position of the main piston. The main piston requires a minimum force of 35 N to actuate the open position of piston due to the frictional force between the main piston and the body and the compression force from the main spring. Hence, a minimum pressure of 3 bars from the inlet is used to apply a force to the main piston to open it at a high temperature. The small piston provided in the pilot passage controls the flow of the pilot pressure water when the temperature changes. The NiTinol spring and the small spring are used to actuate the small piston when the temperature changes. The deflector fixed in front of the output port is used to spray the pressurized water widely. Figure1 shows the closed position of a fire sprinkler in which the small spring maintains the closed position of small piston and blocks the pilot port at the ambient temperature.

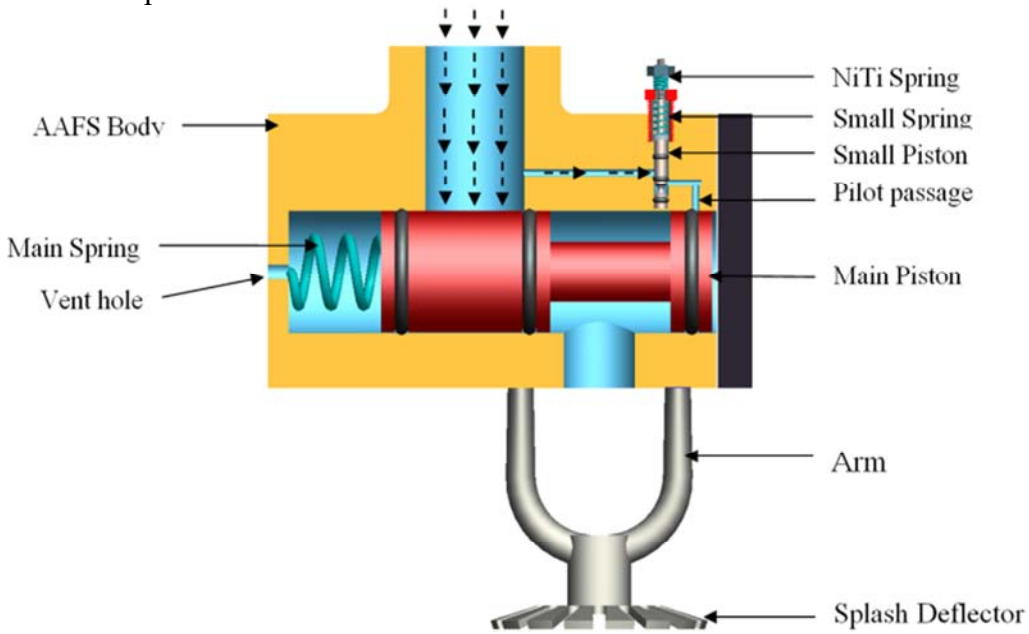

Fig. 1 Closed position of a fire sprinkler

4. Design of a NiTinol actuator

4.1 Low temperature

At a temperature below 62°C, the stiffness of a NiTinol spring is lower (2.380 N/mm) than that of the small spring (4.87 N/mm), hence the small spring compresses the NiTinol spring and makes it pre-strain (expand). Thus, the small spring maintains the closed position of the small piston and stops the flow of pilot pressure as shown in Fig 2.

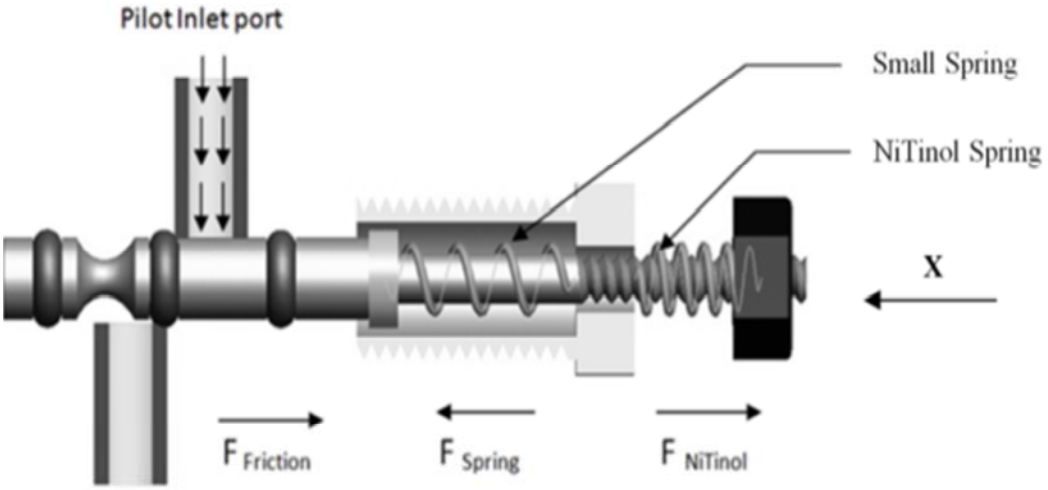

Fig. 2 Position of the small piston at a low temperature

The minimum force required to maintain the closed position of the small piston at normal temperature is

$$F_{NiTinol} + F_{friction} = F_{spring} \tag{1}$$

Since the stiffness of the NiTinol spring depends upon temperature, $K_{NiTinol}$ is defined as

$$F_{NiTinol} = F_M + (F_A - F_M) \times \left(\frac{\theta - \theta_{M_f}}{\theta_{M_s} - \theta_{M_f}} \right) \tag{2}$$

Where F_M, F_A are the forces of the NiTinol spring in the martensite phase and in the austenite phase respectively $\theta_{M_s}, \theta_{M_f}, and\ \theta$ are the experimentally measured temperatures of the martensite start(72°C), the martensite finish (62°C) and of the NiTinol spring respectively. The change in the retaining force of the NiTinol spring from high to low temperature is shown in Fig. 3.

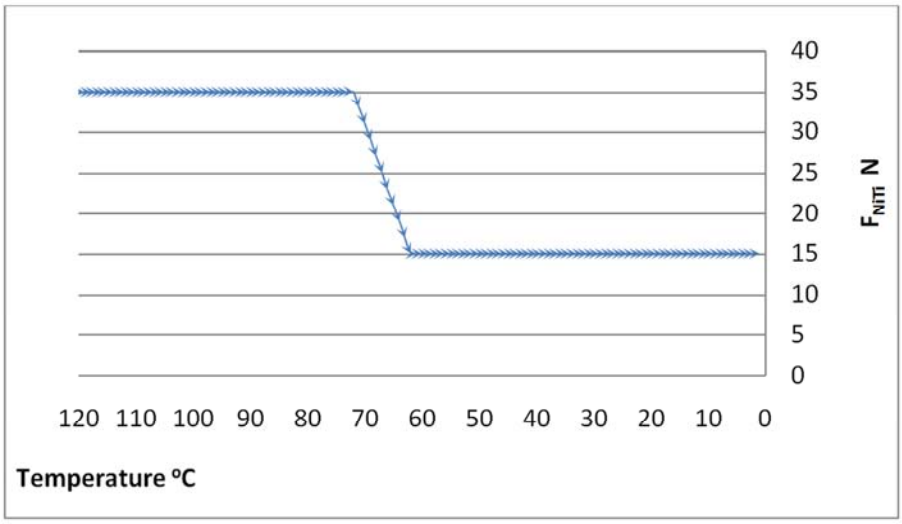

Fig. 3 Retaining force of the NiTinol spring from high to low temperature

$$F_M + (F_A - F_M) \times \left(\frac{\theta - \theta_{M_f}}{\theta_{M_s} - \theta_{M_f}} \right) + F_{friction} = F_{spring} \tag{3}$$

The spring force [24] of a helical spring is $F = \delta \times \left(\frac{Gd^4}{64nR^3}\right)$ (4)

and the relation between Young's modulus and the modulus of rigidity is $E = 2G(1 + v)$. Where G is the modulus of rigidity, d is the diameter of spring wire, R is the radius of spring, n is the active number of coils. F_{spring} is the spring force from the small spring and the required displacement of small piston to open the pilot passage (6mm). Table 1 shows the dimensions and properties of the NiTinol spring, small spring, and the main spring.

Table 1 Specifications of springs

	NiTi Spring @ Martensite	**NiTi Spring @ Austenite**	**Small Spring**	**Main Spring**
Young's modulus ***E***	30 GPa	70 GPa	200 GPa	200 GPa
Rigidity modulus ***G***	11.54 GPa	26.92 GPa	76.92 GPa	76.92 GPa
Diameter of wire ***d***	1.5 mm	1.5 mm	1.2 mm	2 mm
Mean diameter of coil ***D***	8 mm	8 mm	8 mm	12 mm
Number of active coils **n**	6	6	8	20
Spring force ***F***	15 N	35 N	25 N	66 N
Spring stiffness ***K***	2.380 N/mm	5.550 N/mm	4.87 N/mm	4.45 N/mm
Deflection $\boldsymbol{\delta}$	6.31 mm	6.31mm	5.14 mm	14.83

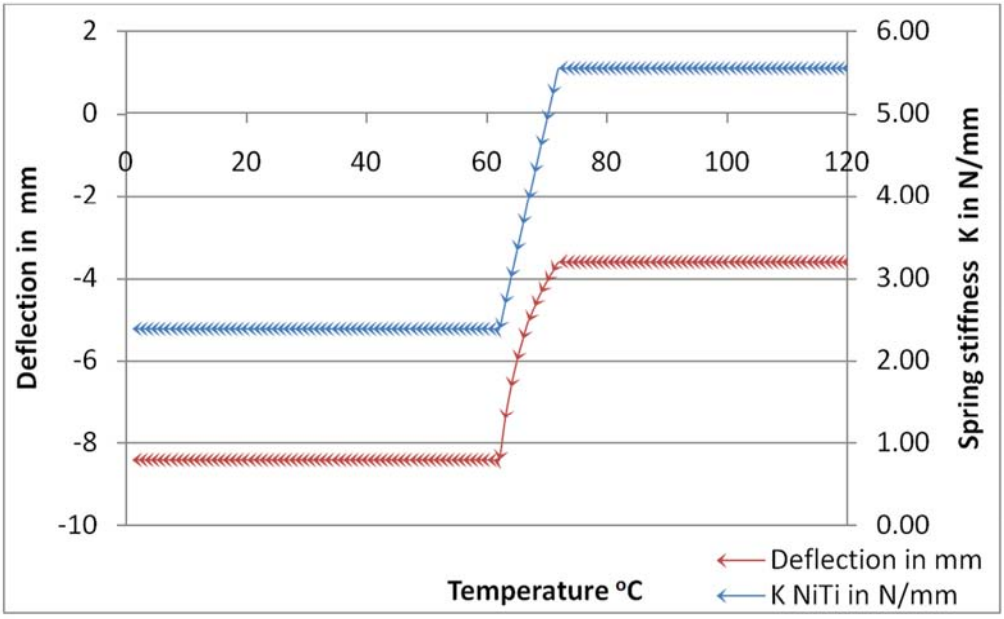

Fig. 4 Changes in the stiffness and deflection of the NiTinol spring from high to low temperature

From Fig. 4one can note that the NiTinol spring gets deflected (compressed) to 4.8 mm due to the change in temperature. This deflection helps to actuate the small piston automatically for closing the pilot passage.

4.2 High temperature

When temperature increases above 88°C, the stiffness of the NiTinol spring increases and exceeds the stiffness of the small spring. Hence, the NiTinol spring tends to return to its

initial shape by compressing the small spring and by actuating the small piston to open position as shown in Fig.5. Thus, the pilot passage gets open and allows the pressurized water to act on the main piston forcing it to open position.

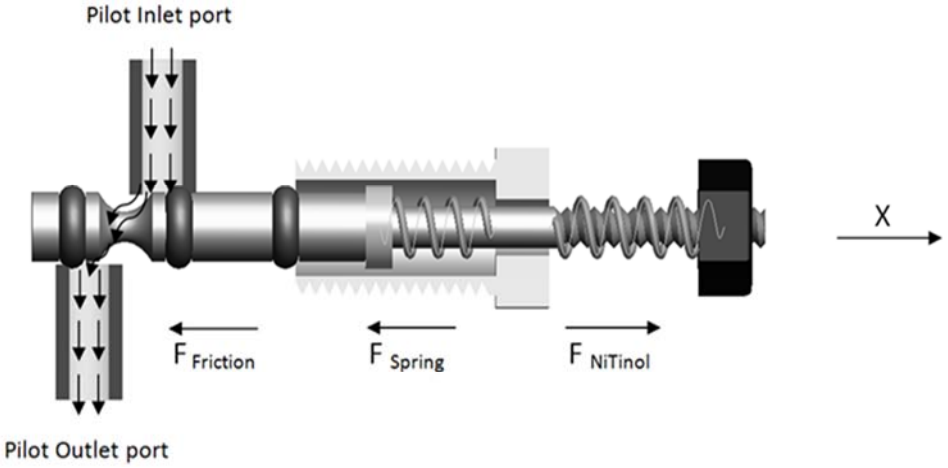

Fig. 5 Open position of the small piston at high temperature

From Fig. 5, the minimum force required to maintain the open position of the small piston at high temperature is

$$F_{NiTinol} - F_{friction} = F_{spring} \tag{5}$$

Since the stiffness of NiTinol spring depends on temperature, $K_{NiTinol}$ is defined as

$$F_{NiTinol} = F_M + (F_A - F_M) \times \left(\frac{\theta - \theta_{A_S}}{\theta_{A_f} - \theta_{A_S}} \right) \tag{6}$$

where K_M, K_A arethe stiffness of the NiTinol spring in the martensite and in the austenite phase. $\theta_{A_s}, \theta_{A_f}, and\ \theta$ are the temperature of austenite start(88°C), austenite finish (98°C) and of the NiTinol spring respectively.

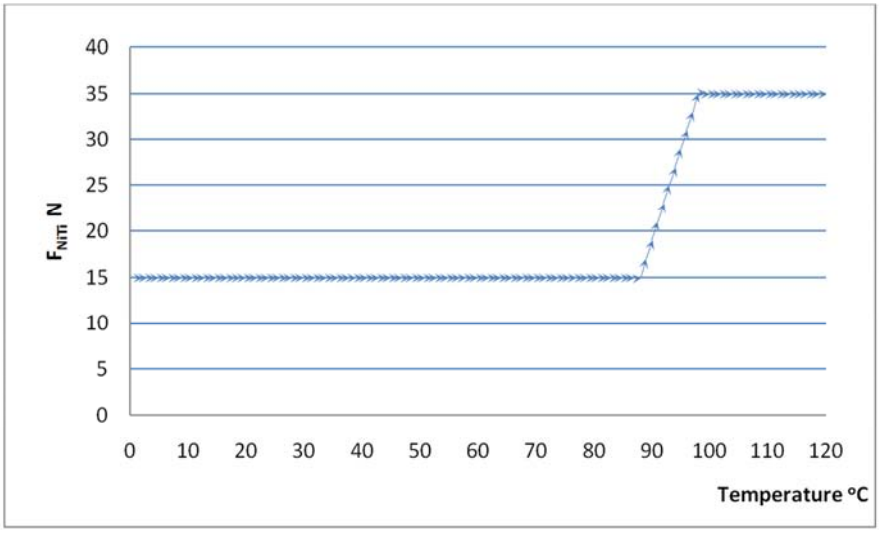

Fig. 6 Change in the retaining force of the NiTinol spring from low to high temperature

Figure 6 shows that the spring force of the NiTinol spring increases gradually from 88°C, and reaches its maximum of 35 N at 98°C. This change in the spring force helps to pull the small piston to open position.

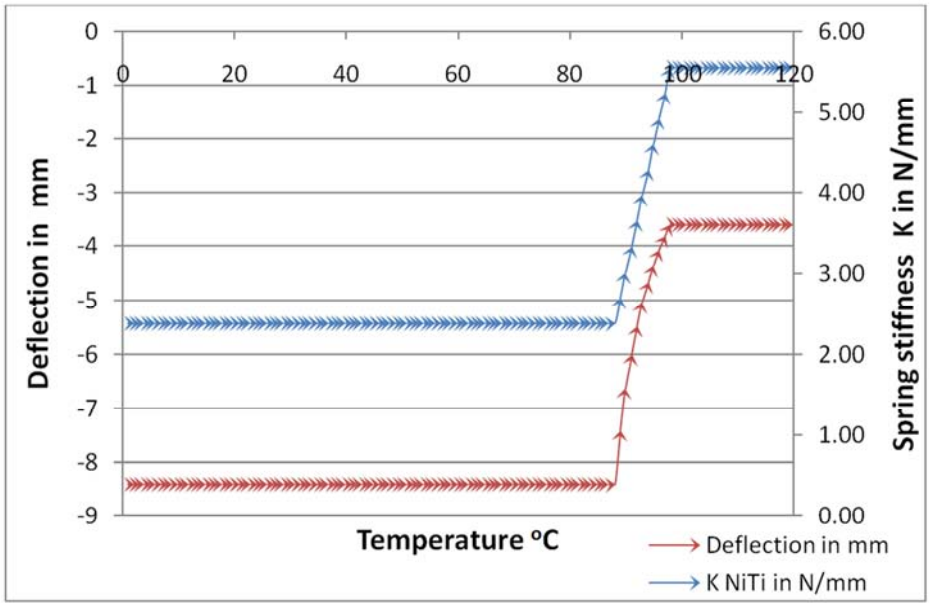

Fig. 7 Changes in the stiffness and deflection of the NiTinol spring from high to low temperature

From Fig. 7 one can note that the NiTinol spring gets deflected (expanded) to 4.8 mm. This deflection helps to actuate the small piston automatically to open position.

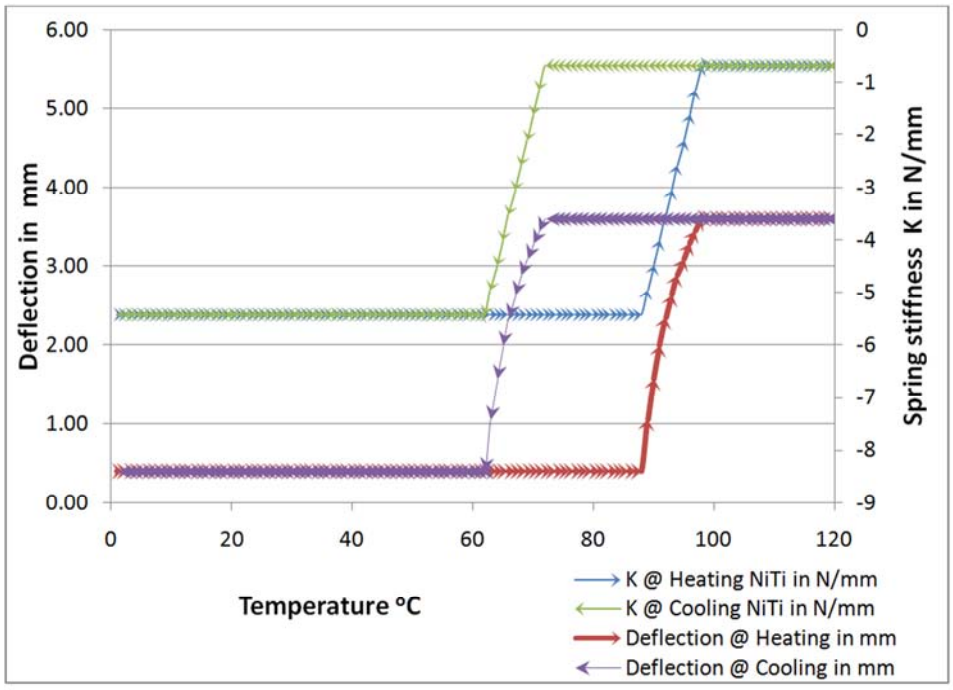

Fig. 8 Hysteresis in stiffness and deflection

Fig. 8 shows the hysteresis effect in stiffness during the change in temperature, which results in a similar hysteresis in deflection.

5. Analysis of a NiTinol spring

A spring was designed in ANSYS APDL and a constant load (8 N) was applied. The change in Young's modulus of SMA with respect to temperature was defined through coding. Then, by varying the temperature of the NiTinol spring, the change in deformation and stress was obtained as shown in Figs. 9 and 10.

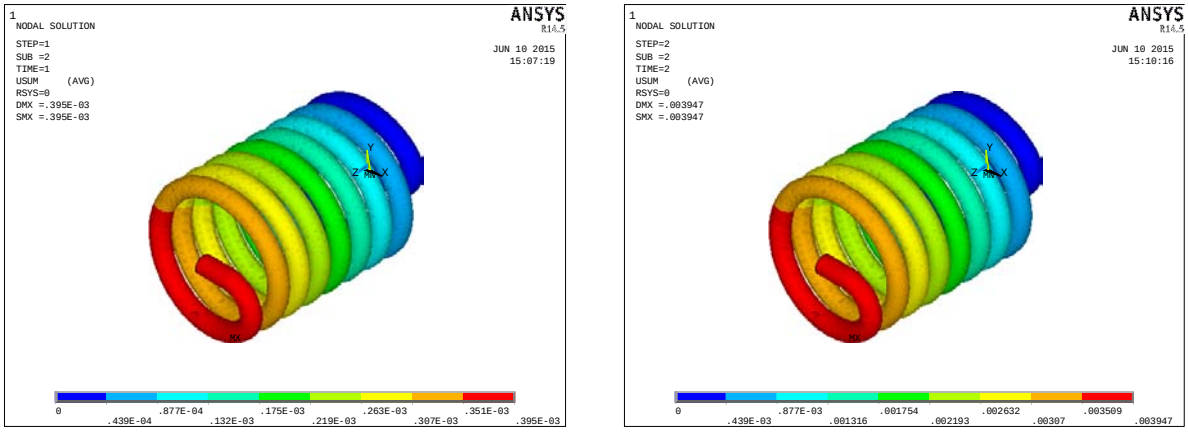

a) b)

Fig. 9 Deformation in the martensite phase (a) and the austenite phase (b)

From Fig. 9 (a) it was found that for the 8 N force applied at a uniform temperature of 30°C (martensite phase) the maximum deformation of the spring is .000395 m. Fig.9(b) shows that at 98°C (austenite phase) the maximum displacement of the spring is .00395 m for the applied force of 8 N. Hence, a 10 mm stroke is obtained in the phase transformation.

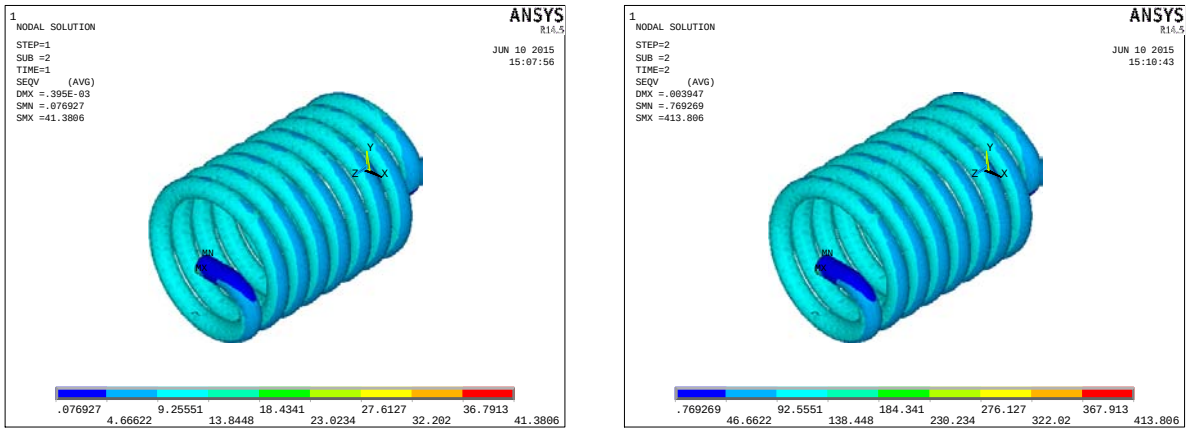

a) b)

Fig. 10 Stress in the martensite phase (a) and the austenite phase (b)

Fig.10 shows the stress developed in the NiTinol spring in the martensite and the austenite phase for the applied force of 8 N. The maximum stress developed in the spring in the martensite phase is 41.38 MPa and in the austenite phase it is 413.81 MPa. This shows that the stress induced in the spring is lower than the ultimate stress (1900 MPa).

6. Shape setting of NiTinol spring

A NiTinol wire of 1.5 mm in diameter is wound into a spring shape around a mandrel and both ends are fixed using lock nuts as shown in Fig. 10. Then the mandrel is kept in furnace at 500°C for 5 minutes and is subsequently hardened by dipping it in cold water.

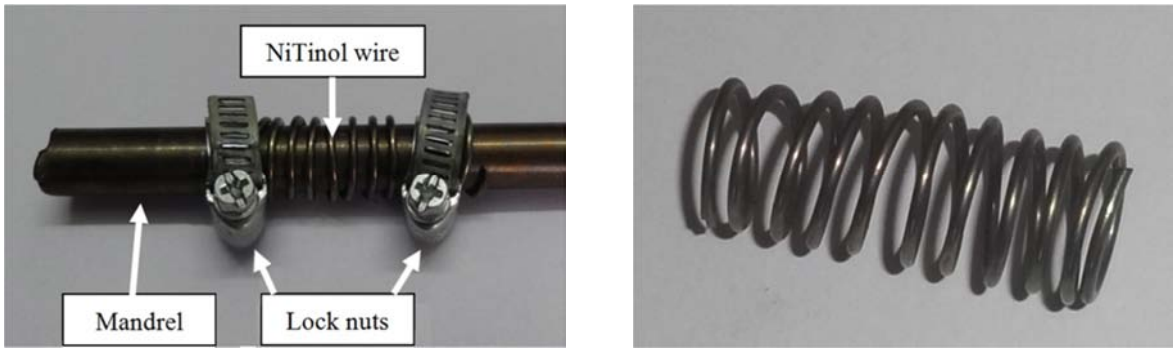

a) b)

Fig. 11 NiTinol spring (mean diameter of 8 mm and the wire diameter of 1.5 mm) made in the shape setting process.

7. Experimental setup

In order to study the recovery force of the NiTinol wire at various temperatures, an experimental setup was created. It consists of a tensile test unit enclosed in a temperature insulated chamber as shown in Fig. 12.

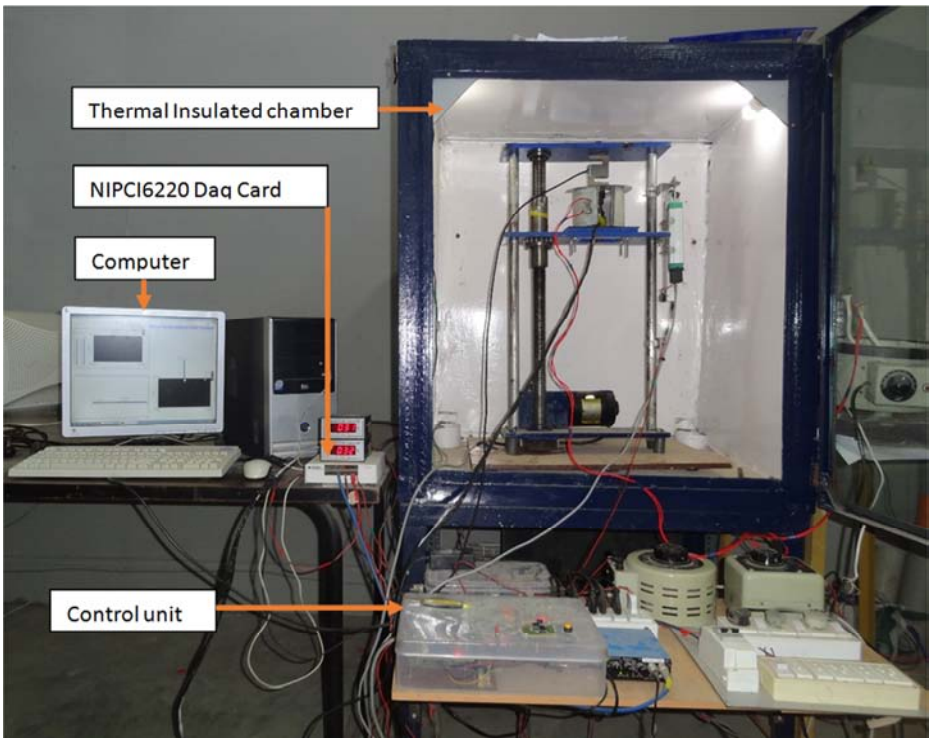

Fig. 12 Experimental setup to study the NiTinol spring properties

An S-type load cell of 100 kg capacity is used to measure the force on the wire and a linear variable differential transformer (LVDT) of 0 to 1000 mm displacement is used to measure the deformation of the wire. The NiTinol wire is fixed firmly between two chucks (one on the fixed top plate and the other on the movable plate). K-type thermocouples are used to measure the temperature of the wire and the chamber. The NIPCI 6220 data acquisition card integrated spring computer helps to capture all experimental data. By using LABVIEW, the data are interrupted. By moving the middle plate upward, the NiTinol spring is compressed to required amounts of strain. By heating the coil, the temperature of the spring is increased uniformly and the respective recovery force is measured.

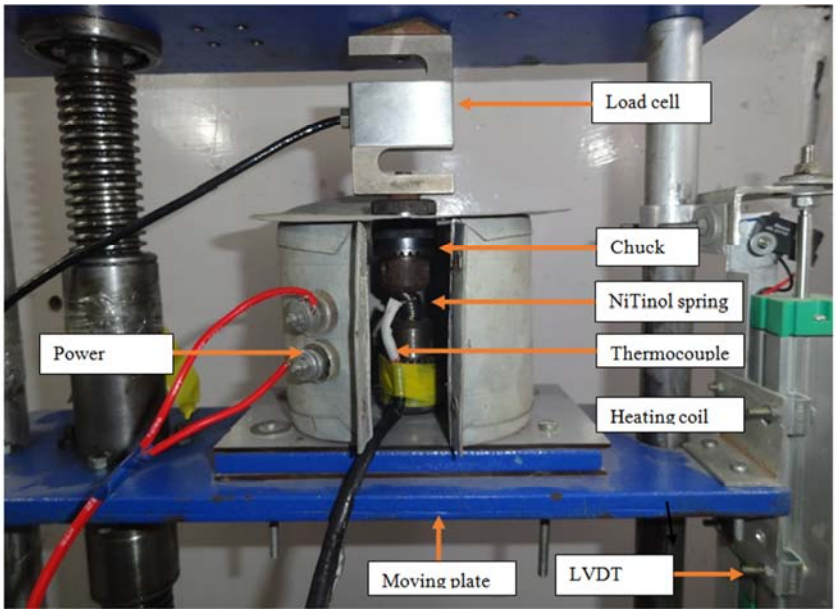

Fig.13 NiTinol spring fixed between two chucks

Figs. 12 and 13 show the experimental setup to study the change in the properties of NiTinol spring with respect to temperature changes. By heating the coil, heat can be generated uniformly for the martensite transformation. A force sensor measures the amount of retaining force. The thermocouple 1 measures the ambient temperature and the thermocouple 2 measures the spring temperature.

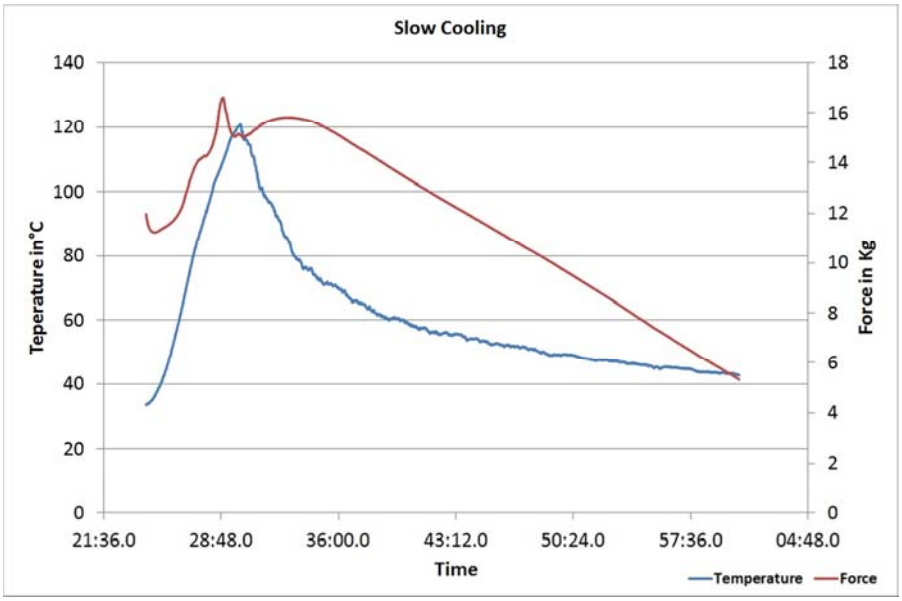

Fig. 14 NiTinol spring in the experimental setup

From Fig. 14 it is clear that the retaining force of the NiTinol spring increased during the transformation phase and then decreased after 120°C due to an increase in dislocation density and the yield strength at maximum strain value [25, 26].

7.1 Minimum pressure required for actuating an AAFS

$$\text{Minimum pressure required to actuate the main piston } (P_{IN}) = \frac{F_{P1}}{A} \quad (5)$$

$$\text{Area of piston } A = \pi r^2 = 3.14 \times 9^2 = 254.34 \text{ mm}^2$$

Minimum force required to actuate the main piston

$$(F_{P1}) = F_{Spring} + F_{Friction} \tag{6}$$

$$F_{Friction} = 10\ \text{N},\quad F_{Spring} = 66\ \text{N}$$

$$F_{P1} = 10 + 66 = 76\ \text{N}$$

$$P_{IN} = 0.2988 \frac{\text{N}}{\text{mm}^2}\ (3\ \text{bar})$$

8. How an AAFS works

8.1 At ambient temperature

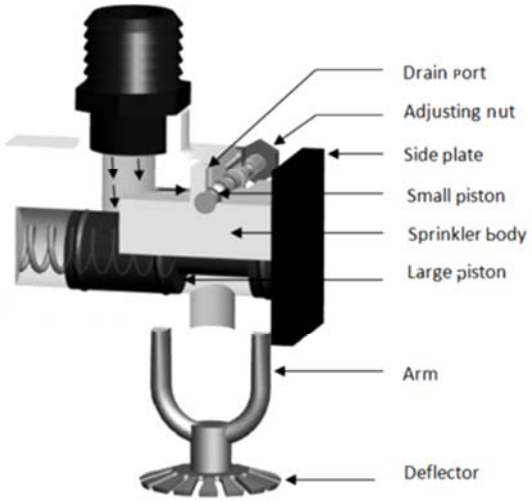

Fig. 15 Close position of an AAFS at low temperature

At ambient temperature, the stiffness of the small spring is higher than that of the NiTinol spring. Hence, the small spring expands by pulling out the NiTinol spring with the small piston. Thus, the pilot passage is blocked and the AAFS is maintained at a closed position as shown in Fig.15.

8.2 At a temperature rise above 88°C

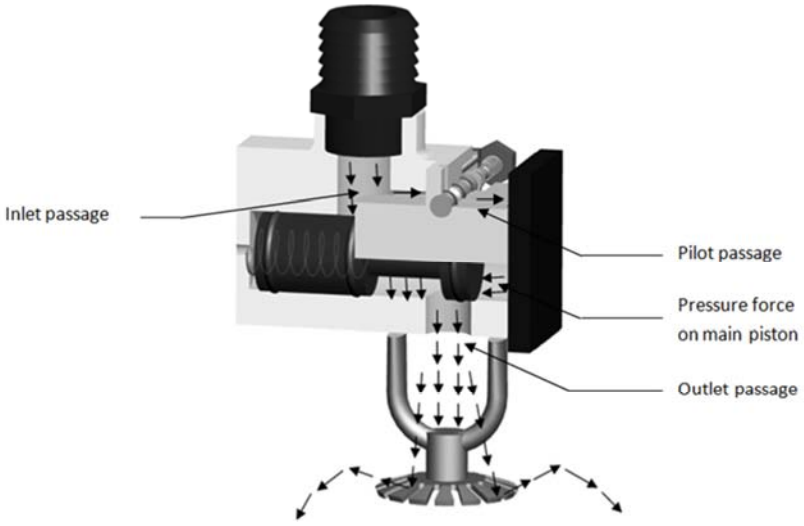

Fig. 16 Open position of an AAFS at a high temperature

When the temperature rises above 88°C, the martensite phase of the NiTinol spring transforms into the austenite phase. As a result, the stiffness of the NiTinol spring rises more steeply than the stiffness of the small spring, which pulls back the small spring and piston and thus opens the pilot pressure port. The pilot pressure acts on the side of the main piston against the main spring and pushes it to open position. Thus, the AAFS gets automatically actuated to open position and sprays out the water in a large radius by passing the pressurized water through the deflector as shown in Fig. 16. When the temperature decreases below 72°C, the austenite phase of the NiTinol spring transforms into the martensite phase. As a result, the stiffness of the NiTinol spring decreases below that of the small spring and the stress on the small spring is reduced so that it returns to the initial position. Thus, the pilot pressure port closes and it opens the drain port. The main spring pushes out the main piston so that the trapped water at the actuation side of the piston drains out through the drain hole resulting in a drop in the pilot pressure to the level of atmospheric pressure.

9. Result

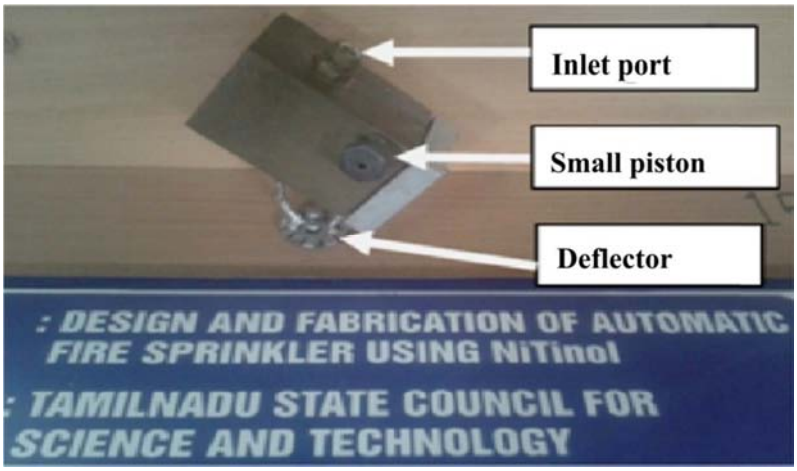

Fig. 17 Fabricated AAFS

The performed experiments showed that the AAFS discharges water at 92°C. The actuation temperature increases due to the temperature difference between the surround and the SMA spring. The AAFS deactivates at the temperature of 57℃ automatically. Adelay in the deactivation temperature is caused by the friction between the sprinkler body and the pistons and by the temperature difference between the surround and the SMA spring.

10. Conclusion

In an AAFS, the retaining force of the NiTinol spring helps to actuate the main piston for discharging water at a high temperature 92°C automatically and to stop the discharge of water when the temperature decreases below 62°C. The double piston arrangement helps to overcome the water pressure acting on the main piston during actuation. The inlet pressure force itself acts as a secondary force to actuate the main piston to open position. By incorporating an AAFS into a fire extinguishing system the water wastage (after fire has been put out) can be reduced, thereby the volume of water storage tank can be reduced. The shape and size of an automatically actuated fire sprinkler can be optimized in further research.

Acknowledgment

The authors would like to thank the Tamilnadu State Council for Science & Technology (TNSCST) for the financial support for this research.

Nomenclature	
K	Stiffness in N/mm
E	Young's modulus in GPa
G	Modulus of rigidity in GPa
A	Area of Cross Section in mm^2
θ	Temperature in degrees Celsius
d	Diameter of spring wire in mm
R	Radius of spring in mm
n	No of active coils in spring
P	Pressure in bar
Subscript and superscript	
eq	Equivalent
M	Martensite phase
A	Austenite phase
Acronyms	
SMA	Shape Memory Alloy
SME	Shape Memory Effect
SE	Super Elasticity
NiTinol	Nickel Titanium/Naval Ordnance Laboratory
AAFS	Automatic actuating fire sprinkler
CFD	Computational Fluid Dynamics

REFERENCES

[1] Mawhinney JR, Hadjisophocleous GV. The role of fire dynamics in design of water mist fire suppression system. Proceedings of INTERFLAM'96, 1996. p. 415–424.

[2] Jinsong Hua, KurichiKumar, BoocheongKhoo, HomgXue. A numerical study of the interaction of water spray with a fire plump. Fire Safety Journal 2002;37:631–657.

[3] Xiangyang Zhou, Stephen PD Aniello, Hong ZengYu. Spray characterization measurements of a pendent fire sprinkler. Fire Safety Journal 2012;54:36–48.

[4] Buddy Clayton Shipman. X- Brace Valve and Flexible Connection for Fire Sprinkles. US Patent 2012; US2012/0298382A1.

[5] James R. Anderson. Concealed Sprinkler Assembly. US Patent 1977; 4014388.

[6] Heinz S. Wolff. Fire Sprinkler with Frangible Body Closing a Flow Passage and Separate Means for Shattering. US Patent 1990; 4896728.

[7] George S. Polan. Sprinkler with Shape Memory Alloy Actuator. US Patent 1996; 5494113.

[8] Marthinus Cornelius. Method and Apparatus for Thermally Actuated Sprinklers. US Patent 2009; US2009/0242218A1.

[9] Alfred Johnson. Frangible Shape memory alloy Fire Sprinkler Valve Actuator. US Patent 2010; US2010/0025050A2.

[10] Tom Goss. Quick Stop Encasement for Malfunction Fire Sprinkler Head. US Patent 2012; US2012/0255629A1.

[11] Hochiki Kabushiki. Sprinkler Head. US Patent 2012; 6073700.

[12] Iyer S S, Haddad Y M. Intelligent materials An overview. International Journal of Pressure Vessels and Piping1994;58:335-344.

[13] Michaud V. Can shape memory alloy composite be smart?ScriptaMaterialia 2004;50:249–253.

[14] MojtabaAzadi, Saeed Behzadipour, Garry Faulkner. Antagonistic variable stiffness elements. Mechanism and Machine Theory 2009;44:1746–1758.

[15] Meng X L, Zheng Y F, Cai W, Zhao LC. Two-way shape memory alloy of a TiNiHf high temperature shape memory alloy. Journal of Alloy and Compounds 2006;372:180–186.

[16] Antonio Vitiello, Giuseppe Giorleo, Renata Erica Morace. Analysis of thermomechanical behaviour of Nitinol wires with high strain rates. Smart Materials and Structures 2005;14:215–221.

[17] Song G, Ma N, Li H-N. Applications of shape memory alloys in civil structures. Engineering Structures 2006;28:1266–1274.

[18] Hashemi S M T, Khadem S E. Modeling and analysis of the vibration behavior of a shape memory alloy beam. International Journal of Mechanical Sciences 2006;48:44-52.

[19] John S, Hariri M. Effect of shape memory alloy actuation on the dynamic response of polymeric composite plates. Composites: Part A 2008;39:769–776.

[20] Anupam Pathak, Diann Brei, Jonathan Luntz. Transformation strain based method for characterization of convective heat transfer from shape memory alloy wires.Smart Materials and Structures 2010;19:35005-35015.

[21] Ras Mathew Y, Ganesh Babu B. Analysis of damping effect of shape memory alloy in active vibration control. Proceedings on International Conference on Thermal Energy and Environment 2011. p. 1837–1842.

[22] Ras Mathew Y, Ganesh Babu B. A study of mechanical behavior of a SMA spring (NiTinol) under constant stress and constant strain. Proceedings on 2nd International Conference on Innovative Research in Engineering and Technology 2013. p. 185-193.

[23] Ganesh Babu B and Ras Mathew Y. Experimental Investigation on Shape Recovery Force of Shape Memory Alloy (NiTinol) at Various Temperatures under Constant Strain. International Journal of Applied Engineering Research 2014; 9 (21):pp. 11353-11364.

[24] WonjunTak, Minsu Lee and Byungky u Kim. Ultimate load and release time controllable non-explosive separation device using a shape memory alloy actuator. Journal of Mechanical Science and Technology 2011; 25 (5): 1141-1147.

[25] R. J. Wasilewski and C. Laboratories. Stress Assisted Martensite Formation in TiNi. ScriptaMetallurgica, vol. 5, pp. 127– 130, 1971.

[26] R. J. Wasilewski and C. Laboratories. Martensitic Transformation and Fatigue Strength in TiNi. ScriptaMetallurgica, vol. 5, pp. 207– 212, 1971.

Submitted: 08.12.2014

Accepted: 10.6.2015

Y. Ras Mathew
rasmmathew@gmail.com
Department of Mechanical Engineering,
Hindusthan College of Engineering & Technology, Coimbatore, India.
B. Ganesh Babu
ganeszbabu@gmail.com
Department of Mechanical Engineering,
Roever College of Engineering & Technology, India.